



Evaluation and Improvement of Eddy Current Position Sensors in Magnetically Suspended Flywheel Systems

Timothy P. Dever
QSS Group, Inc., Brook Park, Ohio

Alan B. Palazzolo and Erwin M. Thomas III
Texas A&M University, College Station, Texas

Ralph H. Jansen
Ohio Aerospace Institute, Brook Park, Ohio

Prepared for the
36th Intersociety Energy Conversion Engineering Conference
cosponsored by the ASME, IEEE, AIChE, ANS, SAE, and AIAA
Savannah, Georgia, July 29–August 2, 2001

Prepared under Contract NAS3-00145

National Aeronautics and
Space Administration

Glenn Research Center

Available from

NASA Center for Aerospace Information
7121 Standard Drive
Hanover, MD 21076

National Technical Information Service
5285 Port Royal Road
Springfield, VA 22100

Available electronically at <http://gltrs.grc.nasa.gov/GLTRS>

Evaluation and Improvement of Eddy Current Position Sensors In Magnetically Suspended Flywheel Systems

Timothy P. Dever
QSS Group, Inc.
Brook Park, Ohio 44142

Alan B. Palazzolo and Erwin M. Thomas III
Texas A&M University
College Station, TX 77843

Ralph H. Jansen
Ohio Aerospace Institute
Brook Park, Ohio 44142

Abstract

Eddy current position sensor performance is evaluated for use in a high-speed flywheel development system. The flywheel utilizes a five axis active magnetic bearing system. The eddy current sensors are used for position feedback for the bearing controller. Measured characteristics include sensitivity to multiple target materials and susceptibility to noise from the magnetic bearings and from sensor-to-sensor crosstalk. Improvements in axial sensor configuration and techniques for noise reduction are described. **Keywords:** eddy current sensor, magnetic bearing

I. Introduction

High-speed flywheel systems are being developed at NASA Glenn Research Center (GRC) in Cleveland, Ohio. Flywheels are a replacement candidate for the batteries currently in use on the International Space Station. Advantages of flywheels over batteries include longer life, higher efficiency and greater depth of discharge. A system level flywheel test bed is operational at GRC. Component level testing is used to evaluate candidate technologies. The flywheel system utilizes active magnetic bearings (AMBs) to provide a long-life, low-loss suspension of the rotating mass. The AMB control system commands power amplifiers, which produce current in the bearing actuators; forces produced by the actuators suspend the rotor. The system utilizes a feedback loop in which the position of the rotor is measured with an eddy current sensor and used as the input to the AMB control algorithm. The sensor is one of the most critical parts of the feedback loop. This paper describes testing of commercially available eddy current sensors in the

flywheel application, to determine sensitivity, sensor-to-sensor cross talk, and susceptibility to electromagnetic interference. Improvements are tested and discussed.

II. Flywheel System Configuration

The flywheel development system configuration is shown in Figure 1. The system consists of a flywheel and a motor/generator mounted on the same shaft. The shaft is suspended using a five axis AMB system. Shaft location for the five axes is determined using non-contact eddy current sensors. The bearing and sensor axes are defined as X1, Y1 (bottom radial direction), X2 and Y2 (top radial direction), and Z (axial direction). When the AMB system is deactivated, the shaft rests on rolling element backup bearings located at the top and bottom of the system.

Nine eddy current position sensors are used in the development system; all are identical. Radial sensing is achieved using two sets of four sensors (top and bottom), and axial sensing is done using a single sensor located at the top of the unit.

Figure 2 shows a top view of the radial eddy current position sensor configuration. In this example, the bottom set of sensors (X1, Y1) is described; the top radial set is similar. The shaft, shown in cross section, is 1.25 in. in diameter. The sensors work in pairs; output from an opposing pair of sensors (e.g. X1 - and X1+) is combined to calculate shaft location on that axis. The typical gap between the shaft and any sensor while the shaft is levitated radially is approximately 60 mils.

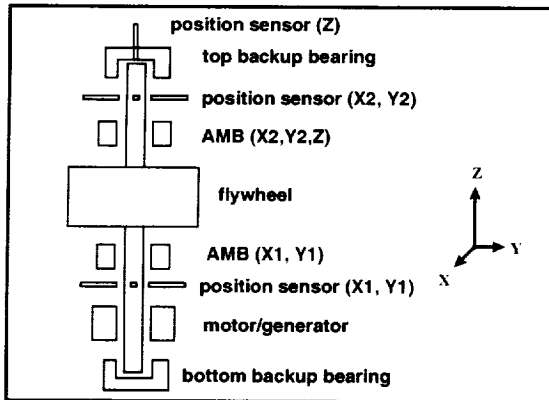


Figure 1. Flywheel Development System.

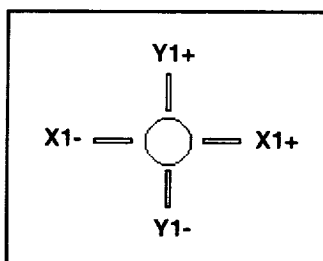


Figure 2. Radial Sensor Configuration.

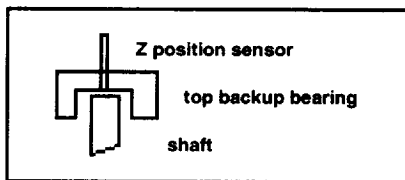


Figure 3. Axial Sensor Configuration.

Figure 3 shows a side view of the Z-axis eddy current position sensor configuration. Axial shaft position is determined by targeting a flat area on the end of the shaft, which the sensor accesses through a clearance hole in the top backup bearing.

A simplified schematic of the AMB control system is shown in Figure 4. The bearing control code generates command signals to allow shaft levitation. These command signals are converted to drive currents by the pulse width modulated (PWM) amplifier, and passed on to the AMB, which alters shaft position. The eddy current sensor signal is processed by the signal conditioning system and fed back to the bearing controller.

Figure 5 depicts the position sensing portion of the AMB controller operator console. Three oscilloscopes are used to provide operator feedback on the position of the flywheel shaft.

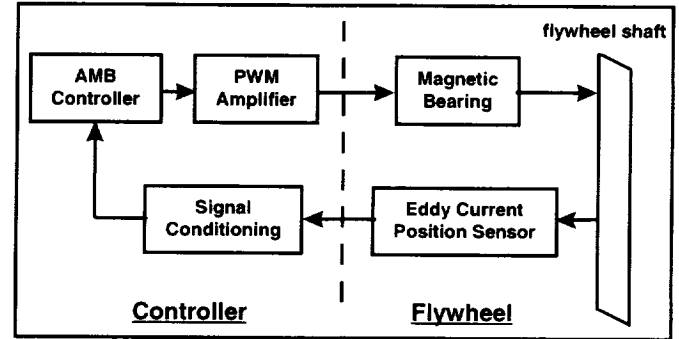


Figure 4. Simplified AMB Control System (one axis).

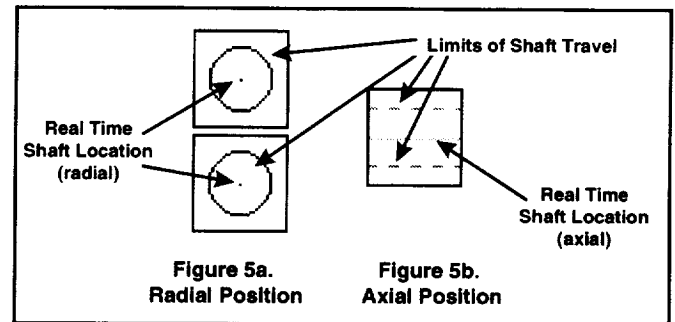


Figure 5. AMB Operator Console - Shaft Position.

For radial levitation control, the operator needs to know the location of the center of the shaft with respect to its available clearance. This is displayed graphically on a polar plot generated on oscilloscopes run in X-Y mode. A circle describing the allowable range of travel of the shaft (defined by the clearance of the backup bearings) is stored in scope memory and continually displayed. Simultaneously, the present center of the shaft (from the X and Y position sensor outputs) is displayed in real time as a dot on the scope. Separate scopes are used to display top and bottom radial shaft position. The radial display layout is shown schematically in Figure 5a.

For axial levitation, the operator needs to know present shaft location in comparison to allowable travel in the axial direction. This is provided by a third oscilloscope, which is run in standard X-T mode. Two cursors mark the top and bottom of the travel allowed by the backup bearings, while the present location of the shaft, determined by the Z position sensor output, is displayed in real time as a trace on the scope. The axial display layout is shown schematically in Figure 5b.

An eddy current sensor has three major components: an oscillator, which generates a radio frequency signal, the sensor, which radiates the signal through the probe tip, and the demodulation circuit, which converts the returned signal into usable form. When a conductive material is placed near the sensor tip, the tip generates an eddy current in the material. The

resulting loss of strength in the return signal is measured and converted by the demodulation circuit into a voltage signal, which is proportional to the gap between the sensor tip and the target. Identical commercially available eddy current sensors were used for all nine sensors.

Commercially available DC brush servo amplifiers were used for the actuators for all five axes. Each of the five PWMs was tuned to match the inductive load of its corresponding bearing coil.

III. Position Sensor Sensitivity

Sensor sensitivity is the ratio of the output voltage change generated by the sensor system to the corresponding change in sensor target position (e.g. 200 mV/mil of target travel). When the shaft of the flywheel in the development system is levitated and centered, the backup bearing clearance allows maximum radial motion of +/- 8 mils, and total axial travel of 22 mils. Of course, for safe and stable operation, the shaft should be kept far away from the backup bearings during rotation, and held by the system precisely. Thus, the position sensor sensitivity must be sufficient to resolve shaft position repeatably to less than one mil, in order for the AMB controller to hold position to the desired tolerance.

Sensitivity of the eddy current sensors was measured for three materials of interest. Results are displayed in Figure 6. This data was generated using a single sensor against flat target samples, setting the gap distance using plastic shims. The slope of the generated lines defines the sensitivity values for each material. By design, the data presented in Figure 6 includes the signal saturation at either end of the linear range of sensor operation. Linear regression was performed on the linear portion of the data, and the resultant sensitivities (line slopes) are presented in Table 1.

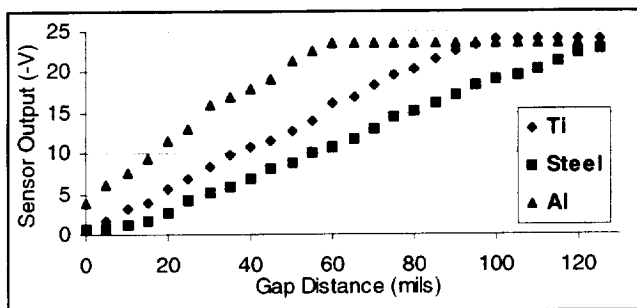


Figure 6. Position Sensor Sensitivity.

Table 1: Sensitivity Data

Target Material	Sensitivity (V/mil)
Steel	0.20
Titanium	0.25
Aluminum	0.34

The manufacturer's published sensitivity for a steel target is 200 mV/mil, which agrees with the measured data for a steel target. The plot displays the extent of the linear range of sensor operation for each material.

A. Radial Sensitivity Verification

The experimental material sensitivity data was taken on flat targets, to minimize target to sensor angle variation errors. However, the radial target in our application is curved. Verification measurements were taken on the development system to ensure that sensitivity to the curved target matches the experimental flat target data.

The upper radial target is made of titanium; two sensors added together to define a radial axis (per Figure 2) should theoretically result in a sensitivity of $2 \times 0.25\text{V/mil}$, or 0.50 V/mil for the radial axis, based on the experimental sensitivity data in Table 1. When the shaft is levitated and centered, the backup bearings limit radial travel of the shaft to +/- 8 mils. The verification test consisted of spinning the flywheel without levitating (so that the shaft ran on the backup bearings), and capturing and storing the radial position sensor output on an oscilloscope. An 8 volt diameter circle was generated, which agrees with the experimental data ($8\text{V} = 16\text{mils} \times 0.50\text{V/mil}$). Therefore, the flat sensitivity data accurately represents sensor sensitivity to a curved target in the system application.

B. Axial Sensitivity Verification

The axial position sensor on the flywheel development unit, as received from the manufacturer, had several problems. It featured a considerable nonlinearity - the effective sensitivity of the sensor system output varied widely depending on axial shaft position. Thus the measured Z position had to be preprocessed in the control code to linearize the signal before passing it on to the AMB control algorithm. Another significant problem was that the X and Y axis motion was not entirely decoupled from the measured Z signal, which caused considerable difficulty in maintaining control stability with increasing flywheel speed.

The axial sensor scheme was redesigned to address the linearity and coupling problems present in the original system. The improved scheme uses a single eddy current Z sensor, and is depicted in Figure 3.

The new scheme was evaluated by first levitating and centering the shaft radially, then stepping shaft position through the entire range of axial travel, from the bottom backup bearing to the top backup bearing. Commanded current and the axial position sensed by the new sensor scheme were measured, and plotted versus the commanded position input to the AMB controller. Figure 7 shows bearing current versus commanded position, and Figure 8 shows displacement measured by the new scheme versus commanded position. The shape of both plots demonstrates that the new axial sensor scheme is very linear;

the need for preprocessing to linearize the axial sensor has been eliminated. The displacement in mils in Figure 8 was calculated by dividing the measured eddy current signal by 0.20 V/mil (the experimentally derived sensitivity for the steel axial target). The total axial travel measured by the system is 22 mils, which agrees with the actual limits of the backup bearing, again verifying the experimentally measured sensitivity data.

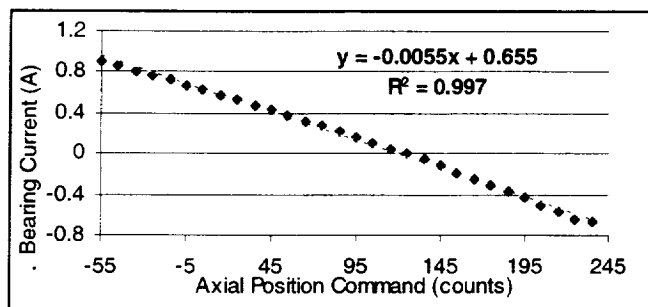


Figure 7. Bearing Current vs. Command (linear region).

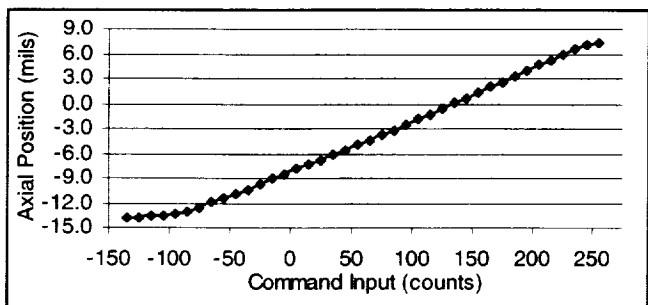


Figure 8. Axial Displacement vs. Command.

In addition to the linearity improvements, operation of the flywheel while spinning has shown that unlike the original sensor system, the new axial sensor measurement is decoupled from shaft motion in the radial direction. This has greatly improved controllability of the system.

IV. Magnetic Bearing Noise

To improve controllability of the AMB, noise sources in the control region should be reduced whenever possible. Since the development flywheel top speed is 60,000 RPM, this means limiting noise from DC to at least 1000 Hz. However, the PWM amplifiers used to drive the AMBs couple switching noise into the position sensors, generating noise in the control region. Although the amplifiers switch at 30KHz, the generated noise is wideband, and simple low-pass filtering is not sufficient to eliminate it. Since this noise is radiated, it cannot be eliminated using sensor line filtering or shielding.

Figure 9 is a plot of the AC portion of the voltage signal on a pair of radial sensors while the flywheel is levitated and centered radially and axially. Note that there is broadband noise within and beyond the control region. This configuration results in noise of 0.5Vpp on the radial sensor signal; at

0.5V/mil this translates to 1 mil of measured position noise using this configuration. This noise level is unacceptable.

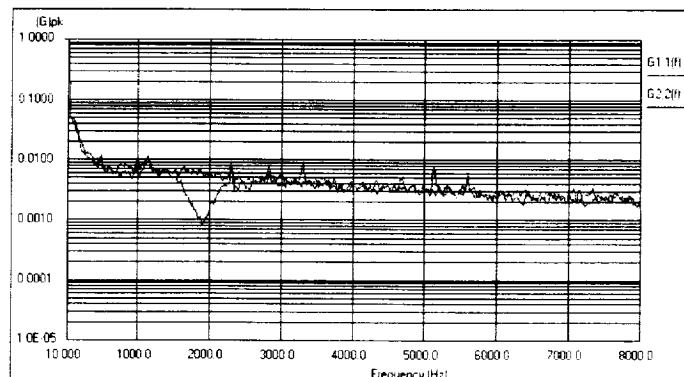


Figure 9. Radial Sensor Output – Levitated Shaft.

The PWM voltage waveform has considerable high frequency content. One approach to decrease the noise coupled into the sensors is to decrease the high frequency content of the PWM voltage waveform. This can be done by adding filters between the PWMs and the AMBs. Commercially available filters, which have a corner frequency of 100 kHz, were added to all five axes of the development system. Figure 10 is a plot of the same two radial AC sensor output signals on the levitated system, with the added filters. Note that the noise floor has decreased dramatically (e.g. by a factor of ~30 at 800 Hz). The sensor noise has been reduced to 0.08Vpp, or 0.16 mils (down from 1.0 mils in the unfiltered system), representing a considerable improvement.

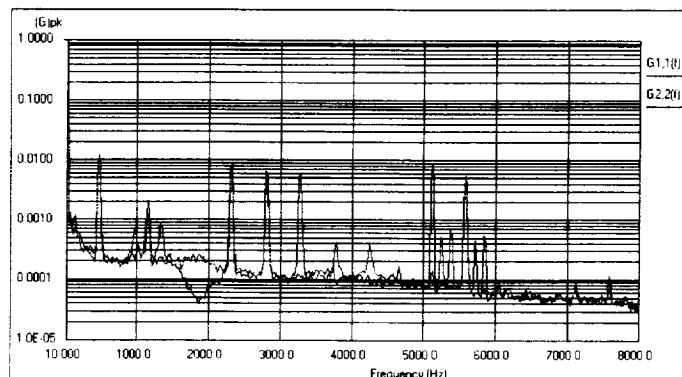


Figure 10. Radial Sensor, Levitated, with PWM Filter.

V. Crosstalk Between Sensors

Sensor-to-sensor crosstalk is another common noise source in eddy current sensors. Slight differences in the drive oscillator frequencies of sensors whose tips are in close proximity to each other can generate beat frequency crosstalk noise in the sensor outputs [1]. This is not a problem with the axial sensor, since it is located far from any other sensors. However, each radial sensor has three other sensors located nearby. Note that when the noise floor dropped due to the

addition of the PWM filters (Figure 10), several large noise spikes were uncovered between 0 and 2 kHz. These spikes are due to sensor-to-sensor crosstalk.

The sensor drive oscillator frequency varies slightly with loading; thus, when the position of the target with respect to the sensor changes, the oscillator frequency for that sensor changes slightly. Since the shaft position can shift slightly during flywheel operation, all of the radial sensor oscillator frequencies can shift as well. Crosstalk noise frequencies are generated by the differences in the operating frequencies of the four oscillators in a radial sensor set; thus, the crosstalk frequencies and amplitudes of the radial sensors change during normal flywheel operation. This makes notch filtering of the crosstalk noise impossible.

Tests to quantify the effects of crosstalk were run on bench top setups to avoid AMB noise interference. First, a pair of sensors was set up at 90 degrees, targeting a 1.25" diameter shaft. This represents a simplified version of the radial sensor configuration (Figure 2). These two sensors, positioned to operate in their linear range, generated a single frequency sine wave crosstalk noise signal. Depending on the relative placement of the two sensors, the resultant noise signal varied in frequency from 200-2000 Hz, and in amplitude up to almost 1 Vpp. With the interaction of four sensors in the system, the character of the noise becomes more complicated.

Next, a bench top mockup of the four sensor radial configuration (see Figure 2) was built. A typical crosstalk spectrum, consisting of the sum of two opposing sensors from this setup (this simulates the sensor output for one radial axis), is shown in Figure 11. Note that multiple crosstalk frequencies exist, several of which are in the control band.

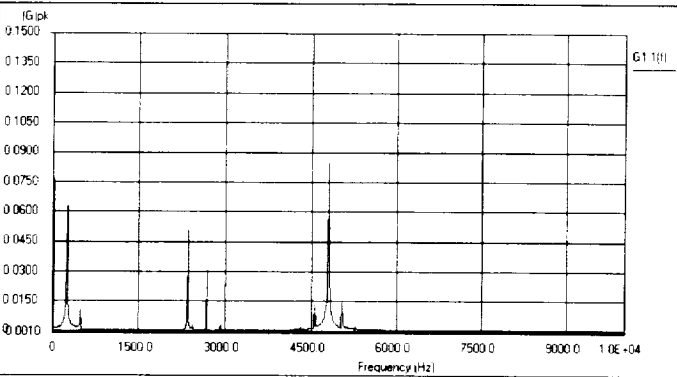


Figure 11. Bench Top Radial Configuration – One Axis.

Adding a small piece of metal near the tip of a sensor loads its oscillator slightly, changing its frequency. Bench top measurements indicate that sensor drive oscillators typically operate at about 1.1 MHz, and adding a shim near the sensor tip changes their operating frequency by about 20 Hz. If two

opposing sensors in the radial configuration are loaded using this technique, a slight frequency difference will be present between any sensor and its two closest neighbors. This can significantly diminish crosstalk noise. Figure 12 shows another spectrum output from the four-sensor bench top setup. The noise from a summed pair of opposing sensors is again displayed; however, this time the two other sensors have been loaded with small metal shims. Note that crosstalk noise has been eliminated in the control band. This shim loading method, while effective, has several drawbacks - sensor sensitivity is decreased significantly, and the process of attaching metal pieces near the tip of the sensor is neither repeatable nor robust.

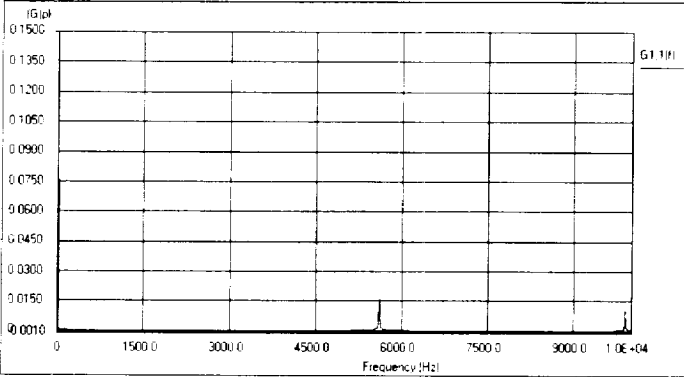


Figure 12. Radial Configuration, Shim Loading – One Axis.

A more practical approach is to load the oscillators electrically. This can be done by adding a parallel capacitance to the lines of a pair of opposing sensors. Testing shows that the addition of 25 pF can change the drive oscillator frequencies by up to 40 Hz. A spectrum of the four-sensor bench setup, this time with two sensors loaded with 25 pF capacitors each, is shown in Figure 13.

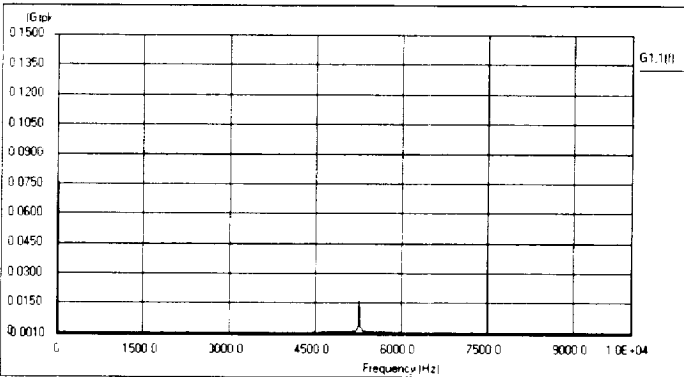


Figure 13. Radial Configuration, Capacitor Loading – One Axis.

Note that, as with the metal shim loading technique, crosstalk noise has been diminished; however, the capacitor approach has several advantages over the shim technique. It is very repeatable, requires no modification of the actual sensor, and has far less impact on the sensor gain. A plot of gain

changes with varying parallel capacitor values is shown in Figure 14. Slight gain changes of this magnitude can easily be corrected for in the signal conditioning system.

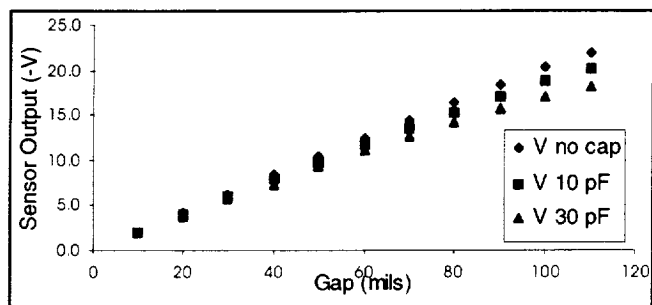


Figure 14. Sensor Gain Changes With Capacitive Loading.

Next, the capacitor loading technique was tested on the flywheel unit. Capacitors (25 pF) were added to a matched pair of radial sensors, and the unit was levitated and centered (identical conditions to those in Figs 10 and 11). The PWM filters were also in place. Results are shown in Figure 15. Note that the noise peaks below 2000 Hz are diminished greatly, showing improvement over the system with the PWM filter only (Figure 10). This configuration further reduces the AC noise on the sensors to about 30 mV, or 0.06 mils; this represents another significant improvement.

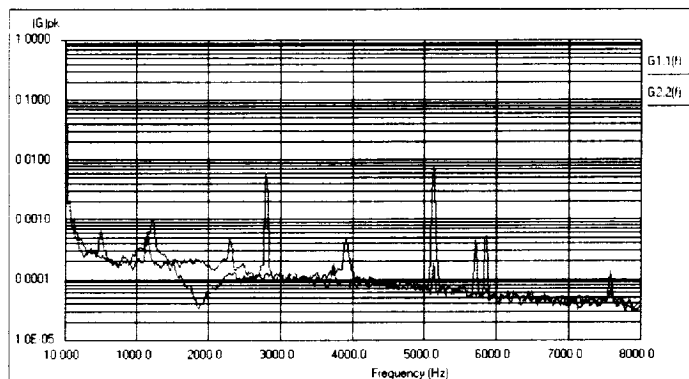


Figure 15. Radial Sensor, Levitated, PWM Filter & Cap Loading.

VI. Conclusions

A new axial eddy current sensor configuration, PWM filters, and capacitive loading of the radial sensors have all been implemented in the flywheel development system. These upgrades have resulted in controllability improvements in both the axial direction (due to improved linearity and reduced cross axis sensor coupling) and the radial directions (due to decreased noise from the PWM and from sensor crosstalk). As a result, system performance has been improved and control system complexity has been reduced, resulting in a more efficient and reliable flywheel system.

VII. References

- [1] Knospe, C.R., and Maslen, E.H., 1999, *Introduction to Active Magnetic Bearings*, 8, pp. 10–11.

REPORT DOCUMENTATION PAGE			Form Approved OMB No. 0704-0188	
Public reporting burden for this collection of information is estimated to average 1 hour per response, including the time for reviewing instructions, searching existing data sources, gathering and maintaining the data needed, and completing and reviewing the collection of information. Send comments regarding this burden estimate or any other aspect of this collection of information, including suggestions for reducing this burden, to Washington Headquarters Services, Directorate for Information Operations and Reports, 1215 Jefferson Davis Highway, Suite 1204, Arlington, VA 22202-4302, and to the Office of Management and Budget, Paperwork Reduction Project (0704-0188), Washington, DC 20503.				
1. AGENCY USE ONLY (Leave blank)		2. REPORT DATE September 2001	3. REPORT TYPE AND DATES COVERED Final Contractor Report	
4. TITLE AND SUBTITLE Evaluation and Improvement of Eddy Current Position Sensors in Magnetically Suspended Flywheel Systems			5. FUNDING NUMBERS WU-755-1A-09-00 NAS3-00145	
6. AUTHOR(S) Timothy P. Dever, Alan B. Palazzolo, Erwin M. Thomas III, and Ralph H. Jansen				
7. PERFORMING ORGANIZATION NAME(S) AND ADDRESS(ES) QSS Group, Inc. 2000 Aerospace Parkway Brook Park, Ohio 44142			8. PERFORMING ORGANIZATION REPORT NUMBER E-12992	
9. SPONSORING/MONITORING AGENCY NAME(S) AND ADDRESS(ES) National Aeronautics and Space Administration Washington, DC 20546-0001			10. SPONSORING/MONITORING AGENCY REPORT NUMBER NASA CR-2001-211137 IECEC2001-ES-20	
11. SUPPLEMENTARY NOTES Prepared for the 36th Intersociety Energy Conversion Engineering Conference cosponsored by the ASME, IEEE, AIChE, ANS, SAE, and AIAA, Savannah, Georgia, July 29-August 2, 2001. Timothy P. Dever, QSS Group, Inc., 2000 Aerospace Parkway, Brook Park, Ohio 44142; Alan B. Palazzolo, Mechanical Engineering Department, and Erwin M. Thomas III, Department of Physics, Texas A&M University, College Station, Texas 77843; and Ralph H. Jansen, Ohio Aerospace Institute, 22800 Cedar Point Road, Brook Park, Ohio 44142. Project Managers, Kerry McLallin, Power and Propulsion Office, NASA Glenn Research Center, organization code 6910, 216-433-5389, and James Soeder, Power and On-Board Propulsion Technology Division, NASA Glenn Research Center, organization code 5450, 216-433-5328.				
12a. DISTRIBUTION/AVAILABILITY STATEMENT Unclassified - Unlimited Subject Categories: 20 and 33 Available electronically at http://gltrs.grc.nasa.gov/GLTRS This publication is available from the NASA Center for Aerospace Information, 301-621-0390.			12b. DISTRIBUTION CODE	
13. ABSTRACT (Maximum 200 words) Eddy current position sensor performance is evaluated for use in a high-speed flywheel development system. The flywheel utilizes a five axis active magnetic bearing system. The eddy current sensors are used for position feedback for the bearing controller. Measured characteristics include sensitivity to multiple target materials and susceptibility to noise from the magnetic bearings and from sensor-to-sensor crosstalk. Improvements in axial sensor configuration and techniques for noise reduction are described.				
14. SUBJECT TERMS Eddy current sensor; Magnetic bearing			15. NUMBER OF PAGES 12	
			16. PRICE CODE	
17. SECURITY CLASSIFICATION OF REPORT Unclassified	18. SECURITY CLASSIFICATION OF THIS PAGE Unclassified	19. SECURITY CLASSIFICATION OF ABSTRACT Unclassified	20. LIMITATION OF ABSTRACT	

